Available online at www.sciencedirect.com

SciVerse ScienceDirect

Scripta Materialia 66 (2012) 13–16

Scripta MATERIALIA

www.elsevier.com/locate/scriptamat

Mechanical length scales and their link to fatigue crack growth kinetics in beta-annealed Ti–6Al–4V

P. Peralta,* T. Villarreal, I. Atodaria and A. Chattopadhyay

Arizona State University, School for Engineering of Matter, Transport and Energy, Tempe, AZ 85287-6106, USA

Received 2 September 2011; accepted 13 September 2011
Available online 24 September 2011

Correlations among microstructure, crack-tip fields and fatigue fracture are studied in beta-annealed Ti–6Al–4V. By means of digital image correlation, the area integral of the opening strain (ε_{int}) over the cyclic plastic zone was obtained, which was proportional to ΔK^m, where m is the Paris exponent, so that $da/dN \propto \varepsilon_{int}$. Analysis shows that $m \cong 2(2 + (1 + n')^{-1})$ where n' is the cyclic hardening exponent ($0 \leqslant n' \leqslant 1$). This predicts $5 \leqslant m \leqslant 6$, in agreement with experiments, and strongly suggests that fatigue fracture of beta-annealed Ti–6Al–4V can be described using non-local strain parameters.

Keywords: Titanium alloys; Fatigue; Fracture; Microstructure; Plasticity

Fatigue crack nucleation and propagation are important damage mechanisms that can control the performance and reliability of metallic engineering structures. Titanium alloys have been used successfully for many critical structural applications because of their high strength, damage tolerance and versatility, since their microstructures and properties can be tailored for particular applications with the appropriate heat treatments [1]. The way in which these different microstructures affect fatigue fracture has been the subject of significant research, which has shown that plastic deformation plays a key role in their crack propagation mechanisms [2–4]. Among Ti alloys, Ti–6Al–4V is widely used in low- and high-temperature applications [1], where it can be found with either a lamellar microstructure, composed of α (hexagonal close packed) and β (body-centered cubic) layers, both of which are essentially ductile, or with a bimodal microstructure, i.e., primary α grains surrounded by α + β lamellar matrix [2]. The lamellar microstructure displays certain advantages over the bimodal one in terms of fatigue performance [2], so understanding the intrinsic mechanisms of fatigue crack growth for that microstructure is of interest in both scientific and practical terms. In that regard, fatigue fracture surfaces in the lamellar structure show striations [3,4]. This, combined with the fact that saturation of hysteresis loops during cyclic deformation has been reported for the lamellar microstructure [3], suggest that plastic blunting, as discussed in Ref. [5], should make an important contribution to fatigue fracture in this material; however, the Paris exponent m reported in Refs. [2] and [4] for the lamellar microstructure is >5, which is beyond the range predicted by many plastic blunting models, i.e., $2 < m < 4$ [5]. In contrast, $m \approx 3.2$ has been reported for the bimodal microstructure [2], which is well within the typical range predicted by plastic blunting for most metallic alloys [5]. Therefore, is likely that additional mechanisms related to the complex lamellar microstructure are present and result in kinetics of fatigue crack growth that cannot be captured by current models of plastic blunting.

Note that most plastic blunting models are based on work for fairly simple materials [5]. Links between plasticity ahead of a fatigue crack and the crack growth kinetics using only plastic blunting arguments are harder to obtain for complex engineering materials owing to the presence of second phases and inclusions, many of them brittle, which produce other damage mechanisms and mask the effects of plastic blunting [5]. However, all the phases in β-annealed Ti–6Al–4V are ductile; therefore, the work presented here focuses on long fatigue cracks in this alloy to draw correlations between microstructure length scales, mechanical length scales, i.e., the sizes of the monotonic and cyclic plastic zones, the strain fields ahead of the fatigue cracks and the kinetics of fatigue crack growth, with emphasis on the potential role of plastic blunting on crack growth

* Corresponding author. Tel.: +1 480 965 2849; fax: +1 480 727 9321; e-mail: pperalta@asu.edu

1359-6462/$ - see front matter © 2011 Acta Materialia Inc. Published by Elsevier Ltd. All rights reserved.
doi:10.1016/j.scriptamat.2011.09.018

kinetics, using the area integral of the opening strain, i.e., the integrated strain ε_{int}, as a parameter for studying these relationships, following Ref. [5]. The goal is to investigate why the Paris exponent in this version of Ti–6Al–4V is larger than those predicted by existing plastic blunting models and find new potential links between plasticity and kinetics of fatigue crack growth in Ti alloys.

The raw material was obtained from a 1/8-in.-thick plate of commercial purity Ti–6Al–4V (6.75% Al max, 4.5% V max, 0.05% N, 0.08% C, 0.2% O, 0.4% Fe). Sections of this plate were annealed in ultrahigh-purity argon, gettered to reduce oxygen levels, for 30 min at 1045 °C, followed by furnace cooling down to room temperature. The cooling rate achieved in this way was fast enough to obtain a coarse Widmanstätten structure, and it was deemed slow enough to provide some stress relief, so no subsequent heating was undertaken. Compact-tension (CT) specimens [6] were machined from these annealed sections using electro-discharge machining (EDM). A notch with ~0.08 mm radius for crack initiation and propagation was also made via EDM. Specimen surfaces were prepared carefully after machining by polishing with 600 and 800 grit SiC paper, followed by final polishing with 0.05 μm 5:1 colloidal silica and 30% hydrogen peroxide solution. Specimens were then etched with an aqueous solution of 2% HF and 10% HNO_3 (by volume) to reveal microstructural features and to provide a pattern for the digital image correlation (DIC) technique to obtain strains ahead of the tip. The microstructure was characterized using optical microscopy, and it was determined that the size of precursor β grains was ~1 mm, the colony size was ~300 μm and the minimum lamellar thickness was ~3 μm. The resulting material had a yield strength of 920 MPa. The geometry of the specimens and the resulting microstructure are shown in Figure 1.

Experimental procedures closely follow those reported in Ref. [5]. Standard fatigue crack propagation experiments were conducted following ASTM E647 [6] in order to quantify the crack growth kinetics of the material and determine the loads to be used for the DIC experiments. The CT specimens were tested under load control in a servo-hydraulic frame with a digital controller. A sinusoidal wave was used, with a maximum load resulting in an initial K_{max} of ~8.9 MPa $m^{1/2}$. The load ratio ($R = K_{min}/K_{max}$) used was 0.1, and the frequency was 5 Hz. Changes in crack length were monitored and recorded as a function of cycles, using a digital camera. Load and image information were recorded as functions of the number of cycles.

The crack growth rate da/dN was calculated as a function of ΔK, using the seven-point incremental polynomial method recommended in ASTM E-647 [6]. This allowed the Paris regime to be identified and the parameters of the power-law to be quantified. The results are shown in Figure 2, along with data from Refs. [2] and [4] for $R = 0.1$ to insure that the heat treatment resulted in crack kinetics consistent with literature reports for the same microstructure.

A power-law fit was done combining data from this work and with those from Ref. [2] to get an average value over the overall range where power-law behavior applies, i.e., for ΔK values slightly above the threshold reported in Ref. [2], i.e., 6 MPa $m^{0.5}$ and above. Data from Ref. [4] are slightly offset, indicating a higher ΔK threshold, but the exponents of all the power law fits agree fairly well with $m \approx 6$. Results indicate that the chosen heat treatment resulted in fatigue fracture behavior consistent with published results on β-annealed Ti–6Al–4V.

Values > 6 MPa $m^{0.5}$ were chosen for the DIC experiments to be well within the power-law regime, and two samples were tested for each load condition. The stress intensities used and the corresponding cyclic and monotonic plastic zone sizes (PZS) estimated from linear elastic fracture mechanics (LEFM) assuming small scale yielding are listed in Table 1.

The in situ experiments to measure crack tip strains required pre-cracking of the samples to grow cracks to a length of >10 mm from the notch tip (half the unbroken ligament). This is ~30 times the measured colony size, and the sample thickness is ~10 times that, so the cracks can be considered "long" [2]. The cracks were propagated under constant ΔK by reducing the load as cracks grew while keeping $R = 0.1$. The procedure kept ΔK within 5% of the target value and insured that a constant PZS was obtained along the crack path [5]. After pre-cracking, specimens were repolished to flatten the surface and etched again, so that the microstructure could provide the speckle pattern needed for DIC [5].

A modified loading stage (see Ref. [5] for details) was used for the in situ experiments. Specimens were mounted on the loading setup, which in turn was fastened to the stage of an optical microscope. Pictures were taken at 10% and 100% of the maximum load at 200×, keeping imaging conditions and the area studied as constant as possible. Before and after pictures were

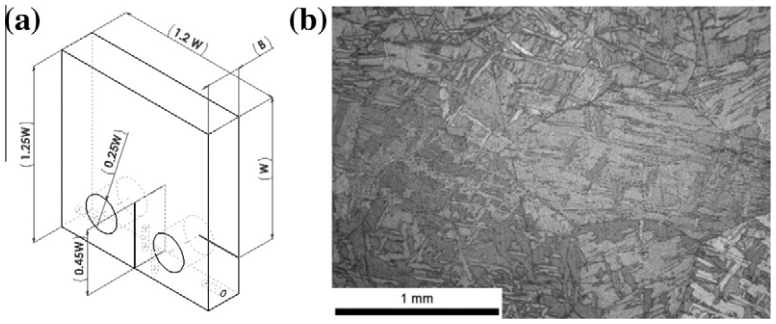

Figure 1. (a) Sample geometry ($W = 25.4$ mm, $B = 3.2$ mm). (b) Microstructure after heat treatment.

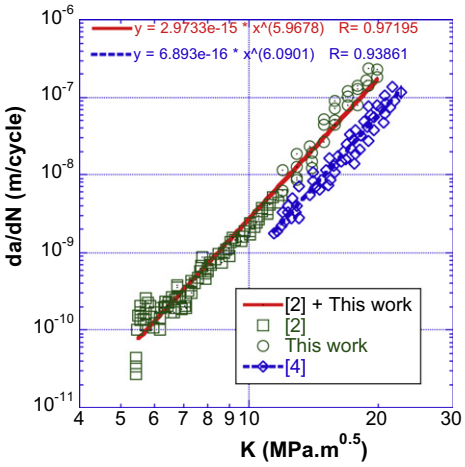

Figure 2. Crack kinetics data for Ti–6Al–4V samples with lamellar microstructure tested at $R = 0.1$ from this work and Refs. [2] and [4].

Table 1. Applied stress intensities and corresponding PZS for in situ experiments.

ΔK (MPa m$^{0.5}$)	K_{max} (MPa m$^{0.5}$)	Monotonic PZS (μm) $r_{p_2}^M = (K_{max}/S_y)^2/\pi$	Cyclic PSZ (μm) $r_{p_2}^C = (\Delta K/2S_y)^2/\pi$
8	8.9	29.7	6.0
15	16.7	104.5	21.2
20	22.2	185.8	37.6

collected for an area of 500 × 500 μm ahead of the crack tips and were analyzed via DIC with the procedures described in Ref. [5].

The full two-dimensional strain fields were obtained from the analysis; however, emphasis was placed on the opening strain, i.e., the normal strain parallel to the load [5]. These fields were used to obtain values for ε_{int} by calculating the area integral of the opening strain over semicircular regions ahead of the tip with radii equal to either r_p^C or r_p^M. Note that both of these mechanical length scales were contained in the pictures used for DIC analysis (see Table 1) and are commensurate with the material's microstructural length scales. This provides the opportunity to study which of these length scales contains the "process zone" ahead of the tip that is responsible for crack propagation by making correlations between ε_{int} obtained for each length scale and the crack growth kinetics. A contour plot of the opening strain field obtained for $\Delta K \approx 15$ MPa.m$^{0.5}$ is shown in Figure 3a. The field has been normalized using the average strain over the monotonic plastic zone of samples tested at 20 MPa.m$^{0.5}$ and has been superimposed on the microstructure. The cyclic and monotonic PZS are also shown. The resulting values of ε_{int} vs ΔK for integration over the cyclic and the monotonic plastic zones are shown in Figure 3b, normalized using the average value of ε_{int} for 20 MPa.m$^{0.5}$.

Note from Figure 3a that the LEFM estimations of the PZS (Table 1) correlated well with a location in the experimental field where the strain started to decrease faster with distance from the crack tip, suggesting that plastic strains indeed dominate the fields close to the crack and that small-scale yielding is a good approximation. This was the case for all three loads used, within the variability expected due to heterogeneity of the local microstructure. Another observation from these results is that maximum strain did not increase substantially with load for $\Delta K > 8$ MPa m$^{0.5}$, but rather it was the area with large strains that increased more rapidly with load. This suggests that a local parameter, like the maximum strain, would not be an appropriate choice to correlate fatigue fracture to applied loads [5].

In particular, the cyclic plastic zone was found to be always contained within a region close to the tip where the strains were not strongly localized along a deformation band (see Fig. 3a), unlike the results shown in [5]. The monotonic plastic zone extended into regions where "lobes" were present, indicating a stronger effect of local microstructure, except for $\Delta K = 8$ MPa m$^{0.5}$. These "lobes" were at angles ranging between ±25° and ±50°, and sometimes came in pairs. As deduced in Ref. [5], where similar results are reported for pure Ni, this suggests that the fields measured here are showing characteristics that, on average, resemble those around a crack in a power-law hardening solid, i.e., the so-called HRR fields [7].

There were difficulties measuring ε_{int} over the cyclic plastic zone for the lowest value of ΔK, as the region was close to the edge of the picture where accuracy is lower. However, comparisons with the monotonic measurement and estimations of the error close to the edge from DIC calculations using the image for the minimum load as both "before and after" pictures led to the conclusion that the value obtained had a reasonable magnitude, but wider error bars.

The results in Figure 3b show that ε_{int} for the monotonic plastic zone follows a power law with an exponent larger than that of the Paris law, which implies that ε_{int} over the monotonic zone grows faster with ΔK than da/dN. One interpretation from a plastic blunting perspective is that the monotonic plastic zone contains strains that help propagate the crack, as well as strains that do not, i.e., kinematically inactive plastic strain [5]. Note that the correlation factor for this power law is ≈0.84, which means that the variability in the measurements, most likely resulting from local strain concentrations at grain boundaries and other microstructural heterogeneities, leads to a less than ideal fit. This is in agreement with the general observations of the variability of the strain field over the outer boundary of the monotonic plastic zone (see Fig. 3a). The value of ε_{int} over the cyclic plastic zone, in contrast, presents a correlation factor ≈0.98, which means that the power law is a good fit to the experimental data, and the exponent of the power law, ~6.1, is quite close to the Paris exponents measured experimentally (see Fig. 2). This implies that ε_{int} obtained over the cyclic plastic zone is approximately proportional to da/dN, which is a conclusion similar to that reached in Ref. [5], and that the strains inside the cyclic plastic zone are indeed responsible for fatigue crack growth. However, a connection between ε_{int} and the Paris exponent cannot be obtained with the same arguments used in Ref. [5], since the strain over the cyclic plastic zone did not localize along deformation

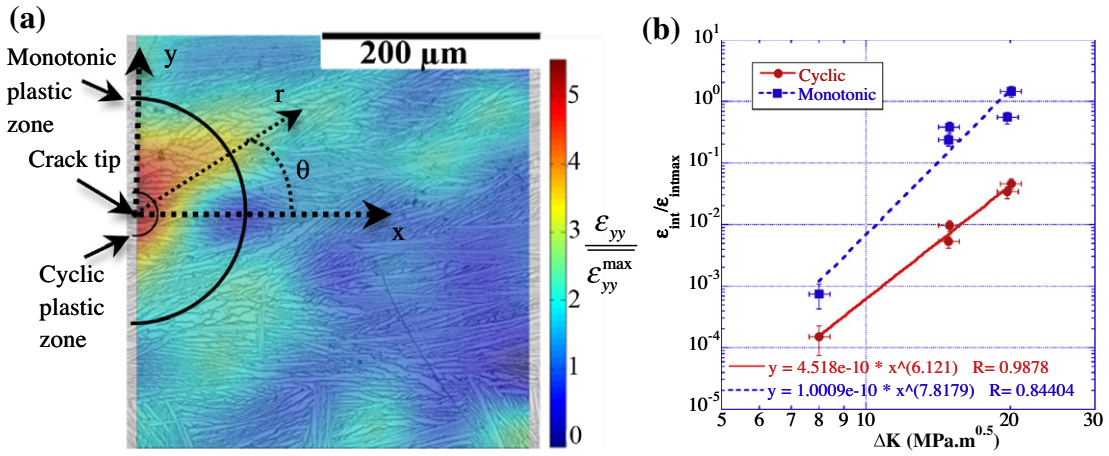

Figure 3. (a) Normalized opening strain field for a sample loaded in situ to $\Delta K \approx 15$ MPa m$^{0.5}$. Cyclic and monotonic PZS are indicated. Load parallel to y. (b) Normalized integrated strain vs ΔK for integration over cyclic and monotonic plastic zones.

bands. Hence, a new analysis must be performed. Using the mean value theorem:

$$\varepsilon_{\text{int}}^{C} = \int_{A_{cyclic}} \varepsilon_{yy} dA = \bar{\varepsilon}_{yy} \pi \left(r_p^C\right)^2 / 2 \tag{1}$$

Assuming that HRR fields hold during the quarter load cycle of the in situ experiment, the strains will be proportional to $J^{\frac{1}{1+n'}}$, where J is the amplitude of the J integral, and n' is the cyclic hardening exponent ($0 \leqslant n' \leqslant 1$) [5]. Furthermore, with $K_{\max} \approx \Delta K$ (since $R = 0.1$), then $J^{\frac{1}{1+n'}} \propto (\Delta K^2)^{\frac{1}{1+n'}}$, since J is path independent. Finally, given that $(r_p^C)^2 \propto (\Delta K)^4$, one obtains

$$\frac{da}{dN} \propto \varepsilon_{\text{int}}^{C} = \int_{A_{cyclic}} \varepsilon_{yy} dA \propto \left(\Delta K^2\right)^{\frac{1}{1+n'}} (\Delta K^4) = \Delta K^{2\left(2+\frac{1}{1+n'}\right)} \tag{2}$$

This implies that da/dN is proportional to $\Delta K^{2\left(2+\frac{1}{1+n'}\right)}$. The exponent in this expression should be the Paris exponent m. Now, given that $0 \leqslant n' \leqslant 1$, then $5 \leqslant m \leqslant 6$. Furthermore, data from Ref. [3] results in $n' \approx 0.02$, which predicts $m \approx 5.96$, in fairly good agreement with experimental crack kinetics measurements (see Fig. 2). This result strongly suggests that plasticity is a key mechanism controlling crack growth kinetics in Ti–6Al–4V.

One final issue to address is the fact that ε_{int} has units of area, but da/dN has units of length. Note that in Ref. [5] the width of the slip bands was used to resolve the issue. In this work, the slip is most likely localized within individual lamellae [8], so that their characteristic length, which does not depend on ΔK, can be used to normalize ε_{int} to obtain a length scale parameter proportional to displacements ahead of the crack tip that preserves the overall dependence on ΔK. A detailed analysis will be presented elsewhere.

In summary, the results indicate that clear connections between the kinetics of crack growth and plasticity can be established for Ti–6Al–4V, using a non-local parameter, ε_{int}. This opens the door to modeling strategies for fatigue crack growth similar to some proposed for fatigue damage accumulation, e.g., the work presented in Refs. [9] and [10], where integrals of fatigue indicator parameters over relevant length scales were used to quantify damage. This work suggests that for β-annealed Ti–6Al–4V the cyclic PZS, which is a function of the applied loads, is the appropriate length scale to evaluate the proposed non-local parameter. Finally, a comparison with Ref. [5] indicates that strain localization (or lack thereof) can play an important role in fatigue crack growth kinetics.

This work was funded by the Multi-University Research Initiative project on Structural Health Monitoring at ASU, under AFOSR Grant FA95550-06-1-0309, David Stargel, program manager. Dallas Kingsbury (ASU) is thanked for his help with fatigue testing.

[1] I.J. Polmear, Light Alloys: Metallurgy of the Light Metals, Butterworth-Heinemann, Oxford, 1995.
[2] R.K. Nalla, B.L. Boyce, J.P. Campbell, J.O. Peters, R.O. Ritchie, Metall. Mater. Trans. A 33A (2002) 899–918.
[3] M. Benedetti, V. Fontanari, Fatigue Fract. Eng. Mat. Struct. 27 (2004) 1073–1089.
[4] X. Wang, Q. Shi, X. Wang, Z. Zhang, Mat. Sci. Eng., A 527 (2010) 1008–1015.
[5] P. Peralta, S.-H. Choi, J. Gee, Int. J. Plasticity 23 (2007) 1763–1795.
[6] ASTM E647: Standard Test Method for Measurement of Fatigue Crack Growth Rates, in Annual Book of ASTM Standards, ASTM, Philadelphia, 2002, pp. 408-438.
[7] M.F. Kanninen, C.H. Popelar, Advanced fracture mechanics, in: A. Acrivos et al., The Oxford Engineering Science Series, vol. 15, New York, Oxford University Press, 1985, p. 563.
[8] F. Bridier, D.L. McDowell, P. Villechaise, J. Mendez, Int. J. Plast 25 (2009) 1066–1082.
[9] M. Shenoy, J. Zhang, D.L. McDowell, Fatigue Fract. Eng. Mat. Struct. 30 (2007) 889–904.
[10] J.D. Hochhalter, D.J. Littlewood, R.J. Christ, M.G. Veilleux, J.E. Bozek, A.R. Ingraffea, A.M. Maniatty, Modell. Simul. Mater. Sci. Eng. 18 (2010) 045004.